

Dual-pulse laser induced breakdown spectroscopy: Time-resolved transmission and spectral measurements[☆]

V. Hohreiter, D.W. Hahn^{*}

Department of Mechanical and Aerospace Engineering, University of Florida, Gainesville, FL 32611, USA

Received 13 December 2004; accepted 16 May 2005

Available online 27 June 2005

Abstract

Spectral analysis of laser-induced plasmas for surface ablation has demonstrated the possibility of analyte signal enhancement with dual-pulse configurations as compared with traditional single-pulse LIBS. Using an orthogonal dual-pulse arrangement, measurements were performed using glass microscope slides to allow both spectral analysis as well as optical transmission measurements. Order of magnitude enhancements in Mg and Si atomic emission signal peak intensities were recorded along with similar enhancements of the continuum emission for dual-pulse LIBS as compared to single-pulse. Peak-to-base measurements showed a roughly 50% increase, while signal-to-noise ratios were enhanced by a factor of 2–3. Temporal analysis of the measured transmitted laser pulse waveforms showed no significant differences between dual-pulse and single-pulse LIBS configurations, providing additional insight into the possible laser coupling processes for the dual-pulse configuration.

© 2005 Elsevier B.V. All rights reserved.

Keywords: LIBS; Plasma; Breakdown; Dual-pulse

1. Introduction

In applications of laser-induced breakdown spectroscopy (LIBS), the ability to measure and clearly resolve individual atomic spectral lines is of fundamental importance. Increasing the effectiveness (i.e. sensitivity and limits-of-detection) of the LIBS technique as a tool for materials analysis implies increasing or maximizing the intensity of the desired atomic emission lines (analyte signal), while decreasing or minimizing the intensity of the measured background emission.

While typical studies utilizing the LIBS technique analyze spectral data generated from a single laser excitation source, researchers have also presented various dual laser or multi-pulse methods. In a dual-pulse configuration, two or more

laser-induced plasmas (temporally separated on the order of nano-seconds to micro-seconds) are created on or near the surface of a solid or liquid sample, as widely reported in the literature [1–19]. In nearly all cases, dual and multi-pulse LIBS systems have resulted in significant increases in the measured atomic emission line intensities when compared to single-pulse systems. Furthermore, the reported increases in emission line intensity are generally accompanied by enhanced ablation of the solid sample (i.e. mass removal rate) when compared with single-pulse LIBS events. The reported multi-pulse phenomenon cannot be explained in the context of total laser energy, as increased emission signals and material ablation rates have been observed in studies where the total energy of a multi-pulse sequence was equal to the energy of a reference single pulse configuration [7]. Recently, atomic emission signal intensities 40 times greater than those of single-pulse LIBS systems, for identical samples, have been reported for dual-pulse experiments [1,8–10].

With one common dual-pulse scheme, an initial “pre-ablation” plasma is created in the air (or general gas matrix) just above the sample surface, usually by aligning the pre-

[☆] This paper was presented at the 3rd International Conference on Laser Induced Plasma Spectroscopy and Applications (LIBS 2004), held in Torremolinos (Málaga, Spain), 28 September – 1 October 2004, and is published in the special issue of *Spectrochimica Acta Part B*, dedicated to that conference.

^{*} Corresponding author. Tel.: +1 352 392 0807.

E-mail address: dwhahn@ufl.edu (D.W. Hahn).

ablation laser beam parallel to the sample surface (i.e. orthogonal configuration). Then on a time-scale of microseconds following the first laser pulse, a second laser, usually aligned normal to the sample surface, is fired such that the pulse passes directly through the pre-ablation laser-induced plasma spark prior to interacting with the target solid surface. The second laser pulse creates the plasma that is ultimately used for spectroscopic analysis similar to all LIBS methodologies. While other configurations have been reported in the papers referenced above, this orthogonal beam, pre-ablation scheme is representative of many dual-pulse implementations, and will serve as the basis for the present study.

While readily implemented, the mechanisms and physics associated with dual-pulse LIBS that account for enhanced signal intensity and material removal rate are not yet clearly understood; although attempts to characterize these underlying processes are the focus of current and ongoing research [3,4]. Furthermore, it should be noted that atomic emission signal enhancement alone is not necessarily a sound metric for evaluating dual-pulse LIBS, namely because if atomic emission and background continuum emission (i.e. recombination and bremsstrahlung processes) are increased proportionally, gains in analyte sensitivity and limit-of-detection may be offset. Because LIBS is generally a technique that is not photon-limited, the benefits of a dual-pulse method (which brings increases in cost and complexity) must be evaluated in terms of analytic figures of merit (e.g. signal-to-noise ratio), as noted for example by Colao, et al. [3].

The present study is concerned with quantifying (through signal-to-background and signal-to-noise measurements) the signal increases observed with dual-pulse LIBS, as well as investigating the physics behind any signal increase through a series of optical transmission measurements and atomic emission spectral analysis, to elucidate the possible role of

the pre-ablation laser spark in the laser coupling processes during the breakdown process.

2. Experimental methods

2.1. Laser system

Two Q-switched Nd:YAG lasers were used for all experiments, and were aligned and configured as shown in Fig. 1. The first laser operated at its fundamental wavelength of 1064 nm with a beam energy of 200 mJ/pulse. The beam was aligned parallel to the sample surface, and was focused with a 200-mm focal length lens to produce an air breakdown and subsequent laser-induced plasma ~ 1 mm above the sample surface. The second laser was frequency-doubled to 532 nm and operated at 100 mJ/pulse. The beam was aligned perpendicular to the sample surface and focused with a 75-mm focal length lens such that the focal spot was formed at the sample surface, where it intersected the beam path of the first, parallel laser. The two lasers were aligned such that their intersecting beam paths resulted in coincident sparks, with the parallel (pre-ablation) air-spark just above the sample surface, and the perpendicular (ablation) spark formed at the sample surface. Both laser Q-switches were externally triggered using a digital delay generator, such that the jitter between the two laser pulses was only a few nanoseconds. The delay generator enabled the two lasers to be fired simultaneously, or have a variable delay introduced between the two pulses.

The sample surface for all experiments was a standard 1-mm thick microscope slide (Corning 2947 Type II Soda Lime Glass). The slide was mounted vertically using a translation stage, such that the slide could be easily

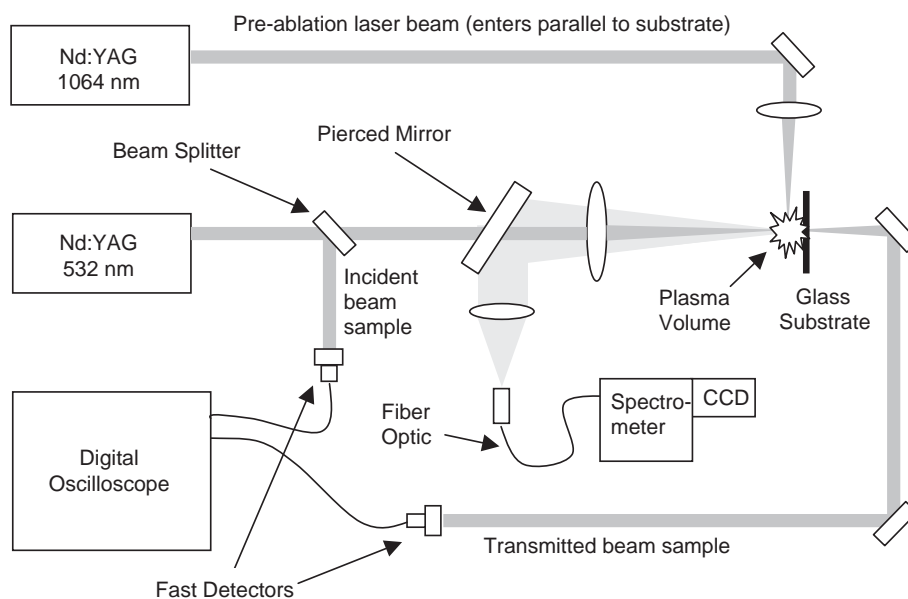


Fig. 1. Experimental apparatus showing LIBS system for both single and dual-pulse operation.

translated to new ablation sites while maintaining precise positioning at the laser focal spot.

2.2. Spectral measurements

Spectral emission from the ablation-spark (i.e. second laser pulse) was collected using a pierced mirror, then focused onto a fiber optic, and finally coupled to 0.275-m spectrometer (Acton SpectraPro-275) and recorded using a 256×1024 element intensified CCD array. A 2400 groove/mm grating was used for dispersion, providing a wavelength region of about 275–305 nm with 0.12-nm spectral resolution.

Spectra were recorded using the single, normally incident 532-nm laser (single laser LIBS), and for the pre-ablation, dual-pulse configuration using delays of 0, 1, 2.5, 5, 10, 20, 50, and 100 μs between the two laser pulses. For all delay experiments, the parallel 1064-nm laser (i.e. pre-ablation laser) was fired first, and the 532-nm laser was fired second for LIBS-based analysis. An external sync from the Q-switch of the 532-nm ablation laser was used to trigger the CCD controller, and for all cases, a delay of 2 μs and a width of 2 μs with respect to this trigger were used for spectral analysis. Data were recorded using an ensemble-average of spectra from 30 consecutive shot-pairs, with each 30-shot sequence initiated on a fresh site on the glass microscope slide, which remained stationary for all 30 shots. The measurements were repeated a total of six times, with each new set corresponding to a new site; hence final spectral data corresponded to an average of 180 laser shots recorded over six sample sites. No attempts were made to quantify any changes in spectral response as a function of shot number, although qualitatively, no significant shot-to-shot differences were noted.

2.3. Transmission measurements

The configuration for the transmission measurements is also shown in Fig. 1. For these experiments, a reference laser pulse waveform was recorded from the incident 532-nm laser using an optical wedge as a beam sampler. The transmitted laser pulse waveform was recorded after passing through the microscope slide. Laser line filters (532-nm) were used in front of fast-response (200-ps rise time) photodetectors to capture the laser waveforms, which were recorded using a digital oscilloscope (2.5 Gigasamples/s). The line filters functioned to minimize broadband plasma emission. Neutral density filters were used to maintain signal linearity for all experiments.

For the transmission measurements, individual waveforms (incident and transmitted pairs) were recorded using delays of 0, 1, 2.5, 5, and 10 μs between the two laser pulses, with the parallel laser (i.e. pre-ablation) preceding the perpendicular ablation laser for all delay experiments, as done for the spectral analysis. Hence the incident and transmitted waveforms corresponded to the ablation laser pulse for all experiments. Due to laser-induced ablation of

the microscope slide, only the first shot-pair was recorded and used for the transmission studies. After the first shot, the resulting ablation crater was found to obscure and scatter subsequent incident laser pulses, rendering the transmission measurement ineffective. Therefore, the transmission data were recorded for the first shot of each fresh glass spot, with this procedure repeated for a total of 20 shots corresponding to each dual-pulse delay setting. For comparison purposes, one set of identical measurements was also recorded for the single 532-nm laser beam.

3. Results and discussion

3.1. Spectral analysis

The Mg I line at 285.21-nm ($0 - 35,051 \text{ cm}^{-1}$) and the Si I line at 288.16-nm ($6299 - 40,992 \text{ cm}^{-1}$) were chosen for spectral analysis due to their strong presence in all shots, spectral proximity to one another, and representation of the glass elemental matrix (73% SiO_2 and 4% MgO for these two analytes). Representative spectra for three experimental cases, specifically dual-pulse delays of 2.5 and 20 μs along with the single-pulse only case, are shown in Fig. 2. A significant increase in both atomic emission line intensity and continuum emission intensity was recorded in all cases of dual-pulse operation with respect to single laser pulse operation, as observed in Fig. 2. Following ablation, the surface of the microscope slide in and around the ablation site was characterized by cracking and pitting, with this behavior observed to increase for the dual-pulse operation.

To quantify the increase in emission signals with the dual-pulse configuration, the peak intensities and the peak-

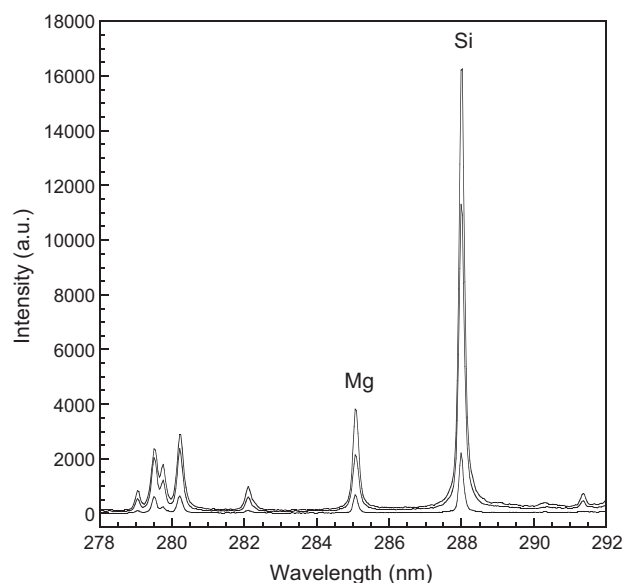


Fig. 2. Spectra showing atomic emission lines of interest, Si I at 288.16 nm and Mg I at 285.21 nm. The spectra correspond to single-pulse LIBS (lower spectrum), dual-pulse LIBS with 2.5 μs delay (middle spectrum), and dual-pulse LIBS with 20 μs delay (top). All spectra have the same scale.

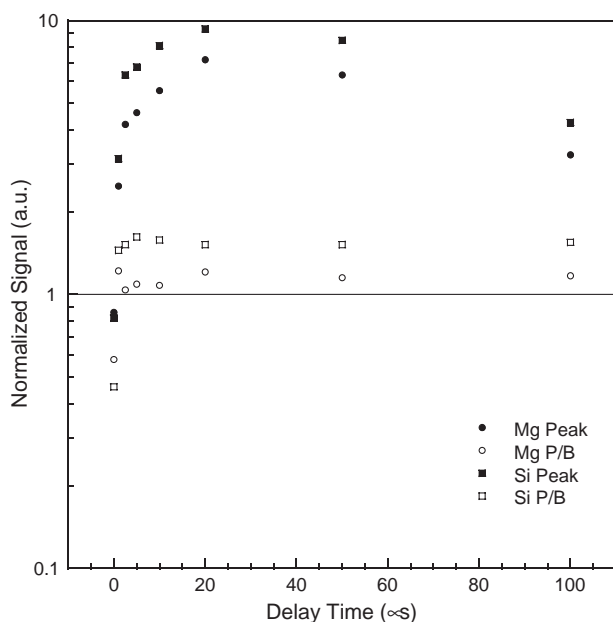


Fig. 3. Spectral atomic emission peak area (full width) and peak-to-base (P/B) measurements as a function of dual-pulse laser delay times. Values are normalized to respective single-pulse data.

to-base (P/B) ratios were calculated for both the dual-pulse operation (delay ranging from 0–100 μs) as well as for the single-pulse case. The peak intensity of the 285.21-nm Mg line increased from a single-pulse value of 3090 counts (arbitrary units) to a maximum value of 22,260 counts at a dual-pulse delay of 20 μs . Similarly, the 288.16-nm Si peak intensity increased from a single-pulse value of 10,710 counts to a maximum value of 99,840 counts at a dual-pulse delay of 20 μs . The greater enhancement in the emission line with higher excitation energy (i.e. Si at $40,992\text{ cm}^{-1}$) is consistent with the results and conclusions reported recently by Gautier et al. [19]. To assess the continuum emission, spectral regions free from atomic emission on either side of the Si and Mg emission lines were used to interpolate the continuum intensity near each peak. Because the continuum emission was found to also increase significantly with the dual-pulse configuration, the resulting peak-to-base (P/B) ratio was enhanced much less than the raw atomic emission peak intensities. Specifically, the P/B values increased by a maximum of 22% and 62% for the Mg and Si emission lines, respectively. Such data demonstrate the close coupling of continuum emission (primarily Bremsstrahlung and recombination) and atomic emission processes in laser-induced plasmas. To better compare the data over the range of dual-pulse delays, the absolute peak intensity and the P/B ratios were all normalized to the respective single-pulse value, with the results plotted in Fig. 3. As observed in the figure, the nearly one order of magnitude increase in atomic emission intensity seen for dual-pulse LIBS is much less dramatic when analyzed in the context of peak-to-base ratios. It is also noted that the normalized results for a dual-pulse delay of zero (i.e. coincident pulses) was less than

unity for both Si and Mg analysis. This result is due to strong absorption of the ablation laser by the pre-ablation plasma, which results from the significant absorption coefficient of the laser-induced plasma within the first few tens of nanoseconds following breakdown, as reported recently [20]. Specifically, transmission measurements revealed an essentially opaque plasma during the period following plasma initiation; hence the pre-ablation, dual-pulse scheme is not realized if the ablation laser pulse is partially shielded from the target by the pre-ablation plasma. Therefore with coincident pulses, the loss of the ablation pulse energy into the pre-ablation laser-induced plasma limits the interaction of the second laser pulse with the target surface, resulting in a lessened analyte response as observed here and also widely reported.

To quantify the analyte response in the context of spectral analysis and figures of merit, the signal-to-noise (S/N) ratio was also calculated for both emission peaks at each delay time. The analyte signal was taken as the full-width integrated emission peak area, while the spectral noise was taken from the root-mean-square (RMS) intensity of the continuum emission adjacent to each peak. The RMS was calculated using an approximately linear continuum region by fitting a least-squares line to the continuum and evaluating the RMS variation with respect to the linear fit. The total noise was the average RMS per pixel multiplied by the width used to integrate the emission line (~ 16 pixels). The S/N ratio of the 285.21-nm Mg line increased from a single-pulse value of 84 to a maximum value of 201 corresponding to a dual-pulse delay of 20 μs . The increase in the 288.16-nm Si line S/N ratio was from 227 for single-pulse LIBS to 700 for the 20- μs dual-pulse configuration. As before, the S/N data were normalized with respect to the single-pulse values, and the results are

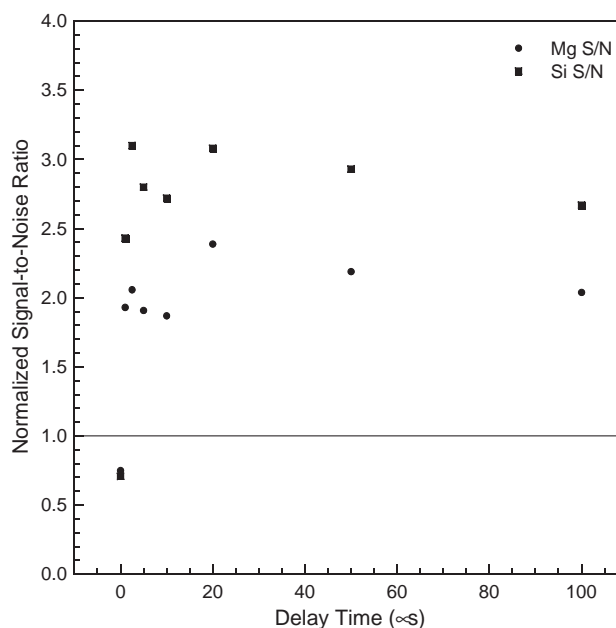


Fig. 4. Signal-to-noise (S/N) ratio as a function of dual-pulse laser delay times. Values are normalized to respective single-pulse data.

shown in Fig. 4. For all non-zero delays, S/N enhancements ranged between a factor of 2 to 3, with the greatest increases occurring for dual-pulse delays between 2 and 20 μs . It is interesting that the S/N ratios fall somewhat between the two limiting cases discussed above, namely the order of magnitude enhancement in raw atomic emission peak intensity, and the minimal enhancements in P/B ratios. Since experimental detection limits and analyte sensitivity directly correlate with the signal-to-noise ratios, such 2 to 3-fold improvements are significant, but must be considered in the context of the added system cost and experimental complexity of a two-laser system.

A few words are noted with regard to the silicon line used for spectral analysis given the large concentration of silicon in the glass slide. Given the moderate level of the lower state of the 288.16-nm transition, namely 6299 cm^{-1} , and the significant transition probability for absorption ($1.75 \times 10^8/\text{s}$), one might expect a non-negligible amount of self-absorption. The silicon lines widths in the present study were essentially constant at 0.17 nm full-width, half-maximum with a relative standard deviation of 5.2% over the various dual-pulse delays, thereby revealing no measurable line broadening. Given the *relative* spectral comparisons of the current study, any self-absorption effects are not considered to affect the present conclusions.

3.2. Temporal analysis

To date, no comprehensive theories exist to explain all the data associated with dual-pulse LIBS, including the reported wide range of enhancements in analyte response as noted above. A primary goal of the current paper is to investigate specific mechanisms that may play a role in dual-pulse LIBS, namely the degree to which the pre-ablation plasma spark results in an enhanced coupling of the second, ablating laser pulse energy into the sample material and laser-induced plasma. Such enhanced laser-material interaction processes may explain increased laser ablation rates and resulting analyte response with dual-pulse LIBS. The transmission measurements were performed to gain insight into such possible mechanisms.

Incident and transmitted laser pulse waveforms were recorded using pristine glass substrates, as described above, for both single-pulse and dual-pulse configurations. For each experimental condition, 20 individual measurements were performed with the resulting waveforms averaged together, noting that each individual shot was recorded on a pristine sample site. Representative waveforms are presented in Fig. 5 for the single-pulse experiments, and for the dual-pulse experiments with delays of 1 and 10 μs , noting that temporal alignment has accounted for the small differences in beam path between incident and transmitted waveforms. For comparison purposes, the incident laser profile is included in Fig. 5, noting that the incident and transmitted waveforms are not presented at the same scale. Two key features may be observed in the Fig. 5 waveforms:

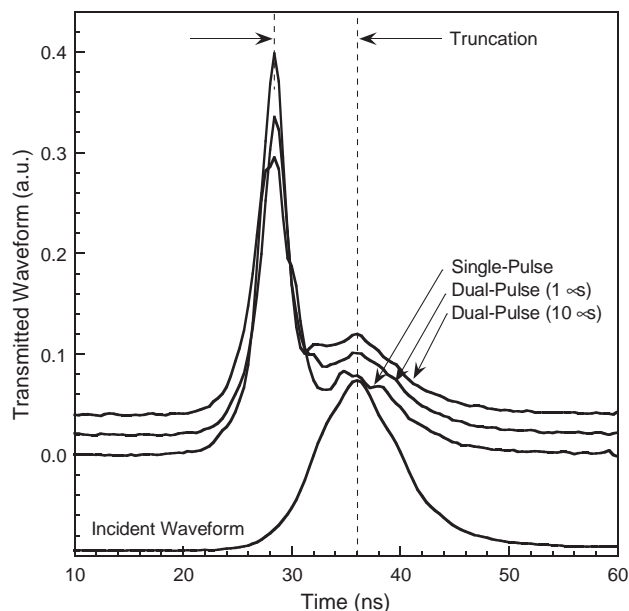


Fig. 5. Average transmitted waveforms showing truncation due to plasma formation. The waveforms correspond to single-pulse LIBS, dual-pulse LIBS with 1 μs delay, and dual-pulse LIBS with 10 μs delay. The three waveforms have the same intensity scale, but have been shifted vertically for clarity. The reference waveform for the incident laser beam is shown for comparison but is not to scale.

first, the single-pulse and dual-pulse waveforms are characterized by essentially indistinguishable profiles, and second, that the transmitted waveforms exhibit a sharp truncation with respect to the incident waveform followed by a secondary local maximum nearly coincident with the peak of the incident waveform. The first observation strongly suggests no significant change in initiation of the laser-induced breakdown process, which will be quantified below. The latter feature demonstrates that following plasma and ablation initiation, there is subsequent strong absorption of the remainder of the laser pulse energy, which is generally attributed to plasma absorption or plasma shielding. The second local maximum has been reported in several other studies [21–23], and is attributed to a brief saturation during the plasma formation/absorption processes near the region of maximum incident intensity.

One may quantify the degree of the attenuation of the incident laser pulse in two ways: (i) by calculating how early in the laser pulse the strong truncation is initiated, and (ii) by calculating the overall transmission of the incident waveform through the surface material. To calculate the first parameter, a truncation time is defined as shown in Fig. 5 as the time difference (Δt) between the maximum of the incident waveform and the maximum of the transmitted waveform. Hence a non-attenuated laser pulse—or a pulse that was uniformly attenuated in time—would yield a truncation time of zero. To calculate the transmission, the integrated peak area of the transmitted waveform was divided by the integrated peak area of the incident waveform. Thus, the fraction of energy from the ablation laser

Table 1
Temporal parameters for single-pulse and dual-pulse LIBS

Laser delay (μs)	Transmission	Truncation (ns)
Single pulse	5.8% (29%)	7.1 ± 1.0
1	5.7% (29%)	7.4 ± 0.90
2	5.3% (26%)	7.3 ± 0.67
5	5.6% (31%)	7.4 ± 0.93
10	5.2% (20%)	7.1 ± 0.98

For the transmission values, the relative standard deviations (RSD) are in parenthesis.

pulse that is transmitted through the pre-ablation spark and the substrate is found.

The truncation time and transmission were calculated for each of the 20 single shot-pair waveforms recorded under each experimental configuration. The results of the transmission measurements and corresponding truncation times are reported in Table 1. The average transmission of the single-pulse data was 5.8% with a relative standard deviation (RSD) of 29%. The average transmission for the dual-pulse experiments ranged from a low of 5.2% (20% RSD) for a delay of 10 μs , to a high of 5.7% (29% RSD) for a delay of 1 μs . As observed in the Table 1 data, no statistically significant change was observed in transmission for any of the delay times during dual-pulse operation as compared with the transmission recorded for the single-pulse LIBS configuration. The experiments reveal that about 95% of the incident laser pulse energy is coupled into system for both dual-pulse and single-pulse configurations under the current experimental conditions. No efforts were made to deconvolve the partitioning of incident energy into the laser-induced plasma and the material ablation process. The finding of constant transmission is significant, as the increased atomic emission signals that accompany dual-pulse operation suggest that a reduced laser pulse transmission through the target (i.e. greater absorption of the ablation laser pulse by the plasmas and/or substrate) may exist for dual-pulse schemes with respect to single-pulse LIBS. No such effect was observed in the current study.

Consistent with the transmission experiments, analysis of the mean truncation times also revealed no statistically significant change between the two LIBS configurations. Specifically, the mean truncation time was 7.1 ± 1.0 ns for the single-pulse experiments, and ranged from 7.1 ± 1.0 ns to 7.4 ± 0.9 ns for the dual-pulse experiments, as presented in Table 1. The difference in integrated area between incident waveforms and transmitted waveforms reveals that, following breakdown, the remaining laser energy is absorbed by the plasma and substrate in combination, with some fraction of the absorbed energy resulting in sample ablation. If the pre-ablation spark of the dual-pulse configuration was enhancing the laser-coupling processes (either laser-material or laser-plasma), a decrease in transmission and/or corresponding change in truncation time should be observed. In contrast, the

present results lead to the conclusion that the initial breakdown and direct coupling mechanisms between the incident laser pulse, the substrate, and the resulting plasma, remain essentially unchanged when comparing single-pulse and dual-pulse configurations. Accordingly, the enhancements in analyte signal and signal-to-noise ratio are likely due to other effects, such as shock-induced reduced pressure, or thermal lensing brought about by the pre-ablation laser spark.

References

- [1] S.M. Angel, D.N. Stratis, K.L. Eland, T. Lai, M.A. Berg, D.M. Gold, LIBS using dual- and ultra-short laser pulses, *Fresenius' J. Anal. Chem.* 369 (2001) 320–327.
- [2] D.A. Cremers, L.J. Radziemski, R.R. Loree, Spectrochemical analysis of liquids using the laser spark, *Appl. Spectrosc.* 38 (1984) 721–729.
- [3] F. Colao, V. Lazic, R. Fantoni, S. Pershin, A comparison of single and double pulse laser-induced breakdown spectroscopy of aluminum samples, *Spectrochim. Acta, Part B: Atom. Spectrosc.* 57 (2002) 1167–1179.
- [4] M. Corsi, G. Cristoforetti, M. Giuffrida, M. Hidalgo, S. Legnaioli, V. Palleschi, A. Salvetti, E. Tognoni, C. Vallebona, Three-dimensional analysis of laser induced plasmas in single and double pulse configuration, *Spectrochim. Acta, Part B: Atom. Spectrosc.* 59 (2004) 723–735.
- [5] S. Nakamura, Y. Ito, K. Sone, Determination of an iron suspension in water by laser-induced breakdown spectroscopy with two sequential laser pulses, *Anal. Chem.* 68 (1996) 2981–2986.
- [6] A.E. Pichahchy, D.A. Cremers, M.J. Ferris, Elemental analysis of metals under water using laser-induced breakdown spectroscopy, *Spectrochim. Acta, Part B: Atom. Spectrosc.* 52 (1997) 25–39.
- [7] R. Sattmann, V. Sturm, R. Noll, Laser-induced breakdown spectroscopy of steel samples using multiple Q-switch Nd:YAG laser pulses, *J. Phys., D. Appl. Phys.* 28 (1995) 2181–2187.
- [8] J. Scaffidi, W. Pearman, M. Lawrence, J. Chance Carter, B.W. Colston, S.M. Angel, Spatial and temporal dependence of interspark interactions in femtosecond-nanosecond dual-pulse laser-induced breakdown spectroscopy, *Appl. Opt.* 43 (27) (2004) 5243–5250.
- [9] J. Scaffidi, W. Pearman, J. Chance Carter, B.W. Colston, S.M. Angel, Effects of sample temperature in femtosecond single-pulse laser-induced breakdown spectroscopy, *Appl. Opt.* 43 (13) (2004) 2786–2791.
- [10] J. Scaffidi, J. Pender, W. Pearman, S.R. Goode, B.W. Colston, J. Chance Carter, S.M. Angel, Dual-pulse laser-induced breakdown spectroscopy with combinations of femtosecond and nanosecond laser pulses, *Appl. Opt.* 42 (30) (2003) 6099–6106.
- [11] L. St-Onge, V. Detalle, M. Sabsabi, Enhanced laser-induced breakdown spectroscopy using the combination of fourth-harmonic and fundamental Nd:YAG laser pulses, *Spectrochim. Acta, Part B: Atom. Spectrosc.* 57 (2002) 121–135.
- [12] L. St-Onge, M. Sabsabi, P. Cielo, Analysis of solids using laser-induced plasma spectroscopy in double-pulse mode, *Spectrochim. Acta, Part B: Atom. Spectrosc.* 53 (1998) 407–415.
- [13] D.N. Stratis, K.L. Eland, S.M. Angel, Enhancement of aluminum, titanium, and iron in glass using pre-ablation spark dual-pulse LIBS, *Appl. Spectrosc.* 54 (12) (2000) 1719–1726.
- [14] D.N. Stratis, K.L. Eland, S.M. Angel, Dual-pulse LIBS using a pre-ablation spark for enhanced ablation and emission, *Appl. Spectrosc.* 54 (9) (2000) 1270–1274.
- [15] D.N. Stratis, K.L. Eland, S.M. Angel, Effect of pulse delay time on a pre-ablation dual-pulse LIBS plasma, *Appl. Spectrosc.* 55 (2001) 1297–1303.

- [16] V. Sturm, L. Peter, R. Noll, Steel analysis with laser-induced breakdown spectrometry in the vacuum ultraviolet, *Appl. Spectrosc.* 54 (2000) 1275–1278.
- [17] E. Tognoni, V. Palleschi, M. Corsi, G. Cristoforetti, Quantitative micro-analysis by laser-induced breakdown spectroscopy: a review of the experimental approaches, *Spectrochim. Acta, Part B: Atom. Spectrosc.* 57 (2002) 1115–1130.
- [18] J. Uebbing, J. Brust, W. Sdorra, F. Leis, K. Niemax, Reheating of a laser-produced plasma by a second pulse laser, *Appl. Spectrosc.* 45 (9) (1991) 1419–1423.
- [19] C. Gautier, P. Fichet, D. Menut, J.-L. Lacour, D. L'Hermite, J. Dubessy, Quantification of the intensity enhancements for the double-pulse laser-induced breakdown spectroscopy in the orthogonal beam geometry, *Spectrochim. Acta, Part B: Atom. Spectrosc.* 60 (2005) 265–276.
- [20] V. Hohreiter, J.E. Carranza, D.W. Hahn, Temporal analysis of laser induced plasma properties as related to laser-induced breakdown spectroscopy, *Spectrochim. Acta, Part B: Atom. Spectrosc.* 59 (3) (2004) 327–333.
- [21] C.V. Bindhu, S.S. Harilal, M.S. Tillack, F. Najmabadi, A.C. Gaeris, Laser propagation and energy absorption by an argon spark, *J. Appl. Phys.* 94 (2003) 7402–7407.
- [22] C.V. Bindhu, S.S. Harilal, M.S. Tillack, F. Najmabadi, A.C. Gaeris, Energy absorption and propagation in laser created sparks, *Appl. Spectrosc.* 58 (2004) 719–726.
- [23] V. Hohreiter, A. Ball, D.W. Hahn, Effects of aerosols and laser-cavity seeding on spectral and temporal stability of laser-induced plasmas: applications to LIBS, *J. Anal. At. Spectrosc.* 19 (2004) 1289–1294.